Proc. Natl. Acad. Sci. USA
Vol. 93, pp. 6382–6386, June 1996
Developmental Biology

Positive genetic feedback governs cAMP spiral wave formation in *Dictyostelium*

HERBERT LEVINE, IGOR ARANSON*, LEV TSIMRING, AND THAI VIET TRUONG†

Institute for Nonlinear Science and Department of Physics, University of California at San Diego, La Jolla, CA 92093-0402

Communicated by Leo P. Kadanoff, University of Chicago, Chicago, IL, February 29, 1996 (received for review January 2, 1996)

ABSTRACT **The aggregation stage of the life cycle of *Dictyostelium discoideum* is governed by the chemotactic response of individual amoebae to excitable waves of cAMP. We modeled this process through a recently introduced hybrid automata-continuum scheme and used computer simulation to unravel the role of specific components of this complex developmental process. Our results indicated an essential role for positive feedback between the cAMP signaling and the expression of the genes encoding the signal transduction and response machinery.**

Upon starvation, *Dictyostelium* amoebae turn on a genetic program, leading to the formation of aggregates, migrating slugs, and eventually fruiting bodies (1). Aggregation is controlled by nonlinear waves of cAMP that propagate through the colony and "inform" individual cells as to the direction to move toward the nearest aggregation center (2). Often, these waves take the form of rotating spirals that are familiar from the study of excitable chemical media such as the Belusov–Zhabotinsky reaction (3) or the catalysis of carbon monoxide on a platinum surface (4). These cAMP waves can either be seen by direct methods (5) or inferred based on cell response visualized by darkfield microscopy (6).

Many authors have published darkfield images from the early aggregation stage of *Dictyostelium* (for example, see refs. 2 and 6). These wave patterns, believed to be initiated by occasional random cAMP emission, start out with a rather disordered spatial structure. At some point, the systems makes a transition to a state with large wavelength spirals. As time progresses, the spiral wavelength shrinks, leaving the system with large domains, each of which is controlled by a coherent spiral wave. Of particular note is that these patterns have on average a large domain size as compared with the most natural scale available, that of the spiral core (see below). After some number of hours, the cells begin to move and the dynamics becomes more complex.

The biochemistry of the signal transduction underlying the cAMP waves has been partially elucidated (7). It is known that the CAR1 receptor detects an above-threshold concentration of cAMP and causes the activation of adenyl cyclase so as to produce (and secrete) additional cAMP. This emission phase is followed by a refractory period during which the receptor is desensitized (8) and the cell cannot be excited. cAMP is degraded by a phosphodiesterase that is itself secreted by the aggregating cells (9). Of crucial importance for our study is the fact that the rate of expression of many critical aggregation-stage genes (including *carA*, adenyl cyclase, etc.) is not constant over the time scale over which the wave patterns develop. Instead, there is a positive feedback loop in which gene expression is stimulated by the detection of cAMP pulses (10). As we shall see, this dynamical mechanism is essential for the generation of the observed coherent spiral patterns.

The publication costs of this article were defrayed in part by page charge payment. This article must therefore be hereby marked "*advertisement*" in accordance with 18 U.S.C. §1734 solely to indicate this fact.

To model cAMP waves and resultant chemotaxis, we use a recently introduced (11, 12) a hybrid methodology in which the cells are treated as discrete automata and the chemical concentration through continuum differential equations. The chemical dynamics of our model is a simplified caricature of detailed kinetic schemes such as those posited by Martiel and Goldbeter (13) or Tang and Othmer (14). Here, cells can be excited by detecting an above threshold cAMP concentration; subsequently, they emit cAMP and proceed into an absolute refractory period after which they can be re-excited. It is well-known (15) that models of this class exhibit all the generic features of waves in excitable media, including mutual annihilation of impinging wavefronts and curvature dependence of wave speed. In particular, it is straightforward to pick initial conditions that will result in a single rotating spiral (within a chosen computational box) and study thereafter the evolution of the cell density field due to chemotaxis in this wave field. This strategy was adopted in previous simulation studies (11) using this scheme or a variety of related concepts (16–18).

However, a problem arises if one tries to simulate the emergence of signaling patterns from biologically plausible initial conditions. It is relatively easy to obtain small-scale spiral structures if one adds small-scale inhomogeneity to the initial field distributions (E. Cox, personal communication). The system does not progress naturally towards the aforementioned large domain state. Obtaining this progression by incorporating an additional self-regulatory mechanism is the goal of this paper.

MODEL

The model was constructed as described in ref. 11; specifically, the cAMP concentration obeys the equation

$$\frac{dC}{dt} = D\nabla^2 C - \Gamma C + \text{sources};$$

the cells are treated as automata that act as the sources in the above equation when excited by an above-threshold chemical signal. After excitation, cAMP emission lasts for some fixed length of time after which the cells enter a refractory period when re-excitation is impossible (the absolute refractory period) or more difficult (the relative refractory period). This threshold value, which we denote C_T, is a critical factor in the signaling dynamics. For a fixed excitable system (such as a set of *Dictyostelium* cells each with a constant level of the signal transduction apparatus), this (normalized) threshold only depends on the time elapsed since the previous excitation; this is incorporated in our simulation by taking C_T to vary continuously from a maximum value C_{max} at the end of the absolute refractory period to a fully recovered value C_{min} after some fixed relative refractory time. In detail, we have

*Present address: Department of Physics, Bar-Ilan University, Ramat Gan, Israel.
†Present address: Department of Physics, University of California, Berkeley, CA 94720.

$$C_T = \left[C_{max} - A\frac{x}{x + T_{ARP}} \right]. \quad [1]$$

Here the time variable x measures time from the end of the absolute refractory period T_{ARP}. The constant A is chosen to make $C_T = C_{min}$ at the end of the relative refractory period $x = T_{RRP}$. The following parameters were used for this simulation: absolute refractory period $T_{ARP} = 8$, relative refractory period $T_{RRP} = 2$, concentration release = 300 over an emission time = 1, $\Gamma \equiv$ cAMP decay rate = 8, $C_{max} = 100$, $C_{min} = 4$. These have been determined phenomenologically by attempting to get our simplified model to produce waves that are qualitatively in accord with observation.

The above model has a set of cells with fixed excitability. In the actual biological system, however, the cells start with some small basal-level expression of signal-system genes; this initial expression is believed to be caused by the accumulation of prestarvation factor (19). Subsequent increases in excitability are caused by the aforementioned positive feedback from the CAR1 receptor; however, this increase depends on the specific (pulsatile) excitation of individual cells and therefore there can be spatial variability induced via this process. This is in distinction to another logical possibility not seen in actual *Dictyostelium*, a uniform increase in excitability whereby each cell would exhibit the same time-dependent excitability. To include this effect, we modify the above equation for the threshold to

$$C_T = \left[C_{max} - A\frac{x}{x + T_{ARP}} \right](1 - E) \quad [2]$$

where we now have a new degree of freedom for each cell, the excitability E. We assume that E obeys the kinetic equation

$$\frac{dE}{dt} = -\alpha E + \beta C \quad [3]$$

as long as E is below some maximal level E_{max}. The crucial term is the positive feedback (governed by the positive constant β) that causes E to increase after the passage of a wave of high cAMP concentration C. Since the concentration C at some cell location is appreciable in magnitude only during the passage of a wavefront over that cell, this equation gives rise to a rate of cell excitability increase that depends on the frequency of the cAMP waves in its vicinity. For completeness, we have included a term reflecting the turnover of signal-system proteins with rate α, but this is not crucial in any of the following.

It is worth commenting on the relationship between our crude feedback model and what actually could be measured in the real system. The gel experiments (essentially messenger RNA levels with and without cAMP pulses) reviewed in ref. 10 are not highly quantitative and in any event do not directly tell us the excitability of the cells. What is needed is an explicit determination of the change in both the cAMP threshold and the cAMP emission parameters for a single received pulse. Since the pulse is rather large and sharp, it is highly likely that the cellular response will be fixed, i.e., independent of the small variations in the pulse structure. In our model, pulses have a fixed shape (at least until the cell density is allowed to change) and hence the response per pulse depends only the parameter β; this would then allow us to determine this parameter. This way of thinking about the feedback, as a sort of map from one pulse to the next, also guarantees that the specific form that we take (linear in C) is not crucial for any qualitative aspect of the model dynamics.

Here we are interested in the establishment of a wave field from an initially featureless state with random firing. Random firing was accomplished by having cells emit cAMP when they reached 15 time units after their previous excitation. The simulation uses explicit time-stepping on a hexagonal grid of size 145 × 167. Most of our results concern what happens before chemotactic motion begins to seriously distort the cell density. When we do want to include cell motion, this is done precisely as described in ref. 11, where cells move one cell diameter per received signal (in the direction of the wave source) as long as they can do so without overlapping some other cell. This algorithm suffices to describe cell motion until such time as cells begin to climb out of the two-dimensional plane of aggregation and form a three-dimensional mound.

RESULTS AND DISCUSSION

We wish to understand the mechanism whereby spiral patterns with a large domain size emerge from the quiescent initial state. To initiate cAMP waves, we assume that some cells "fire" randomly, releasing cAMP. Let us first concentrate on the "constitutive" system, i.e., the model without any genetic feedback but rather one in which all cells start out being fully excitable. The results of one simulation with this assumption (with E fixed at $E_{max} = 0.93$) are shown in Fig. 1; concentric waves indeed propagated outward from the firing sites, but the system did not spontaneously develop coherent spiraling signal patterns. These results were unchanged upon addition of small inhomogeneities in cell density or excitability (data not shown). This wave structure is similar to that seen in low density aggregates that do not form spirals; in these cases, aggregation progresses beyond this stage due to the formation (by chemotaxis) of small clumps that become self-oscillatory and generate repeated concentric patterns.

In Fig. 2, we show a comparison of the full model with genetic feedback to a model with the alternate assumption of the excitability increasing uniformly to its maximal value. In both cases, persistent waves are ignited by the initial random firing. Initially, the excitability is too low for waves to propagate. As the excitability increases, waves occasionally form and

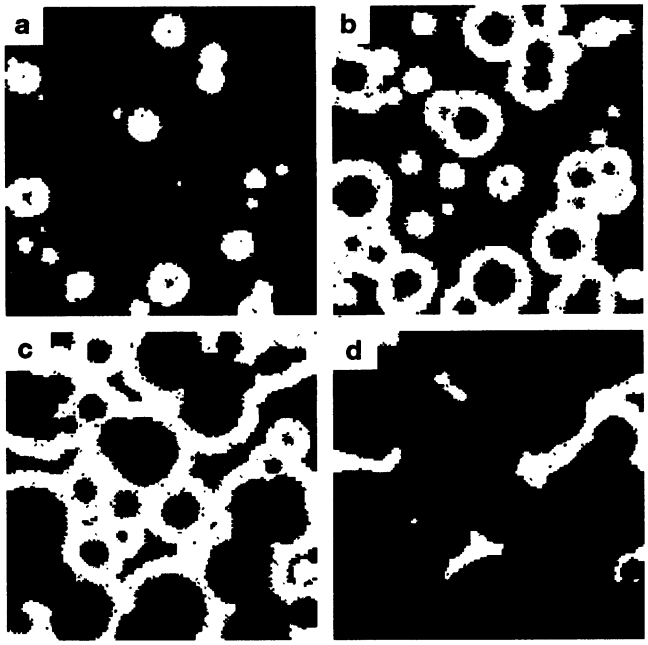

FIG. 1. Time evolution of a concentric wave pattern due to random firing of cells in a system with time-independent excitability. White indicates regions with high level of cAMP concentration; *a*, nondimensional time 50; *b*, 100; *c*, 150; *d*, 250. There is no breaking of the waves due to the uniformity of the receptor state variable of all the cells. After these particular waves die down, new ones will be initiated by the random firings of other cells. Here, the cell density = 0.98.

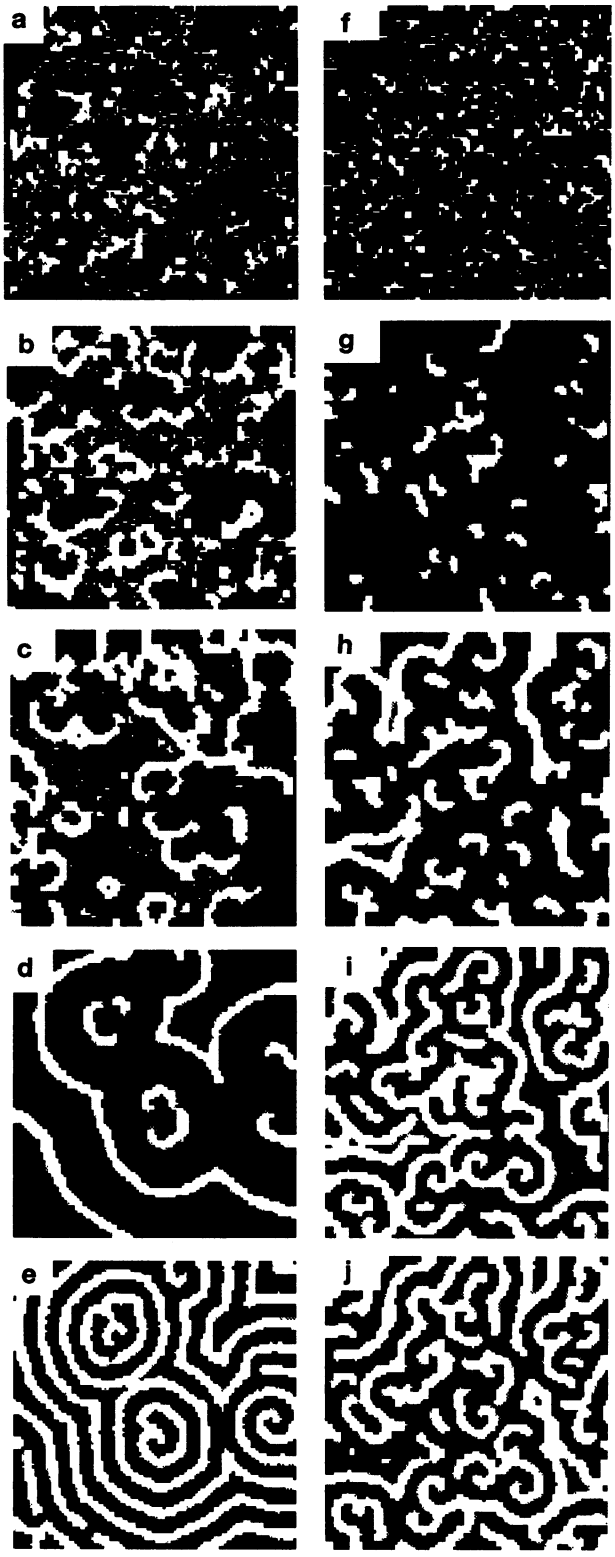

FIG. 2. Comparison of the models with (*a–e*) and without (*f–j*) genetic feedback. (A complete animation of the model dynamics with genetic coupling turned on can be viewed at http://inls.ucsd.edu/~lev/animate/anim-cAMP.html.) Here the excitability is increased in accordance with Eq. **2** with parameters $\alpha = 0.0005$, $\beta = 1.24$, $E_{max} = 0.93$. *f–j* are obtained with a uniform increase in excitability with approximately the same rate as the average cell in *a–e*. Similar results are obtained with $\alpha = 0$ (data not shown). Sequences *a–e* and *f–j* both correspond to nondimensional times 250, 700, 1125, 3500, and 16,500, respectively.

excite some cells. This has the effect of randomizing the cell receptor state (in our model randomizing the time since last firing) and this randomness eventually causes waves to "break" and create spiral tips. This mechanism of spiral formation can also be seen in purely chemical media if the threshold is systematically varied (20). However, the decoupled model did not proceed to organize the initial disordered wave pattern into a coherent set of spiral wave domains. The spatial correlation remained short-ranged, dependent on the precise details of the assumptions regarding initial firing.

The genetically coupled model developed long-range spiral structures independent of the initial state; this is seen in the sequence shown in Fig. 2. In the simulation, large wavelength spirals were formed by competition among smaller spirals (Fig. 2*c*) and then wind up more tightly as excitability increases (Fig. 2*d*), leading eventually to large spiral domains. In the uncoupled model, on the other hand, there was no overall decrease in the number of independent signal centers (nascent spiral cores) and the overall pattern never became ordered. Note that the patterns in both simulations evolved without the need for any additional random firing or for any pacemaker (i.e., self-oscillatory) regions; this criterion is the crucial one for determining the "spiraling" nature of the wave state.

The dynamic process that leads from Fig. 2 *b* to *d* can be thought of as a symmetry-breaking instability, whereby one member of a small spiral pair overwhelms its neighbor and "captures" its "territory." This instability does not occur in any model of excitable systems that had been studied to date and can be traced explicitly (21) to the interaction between the

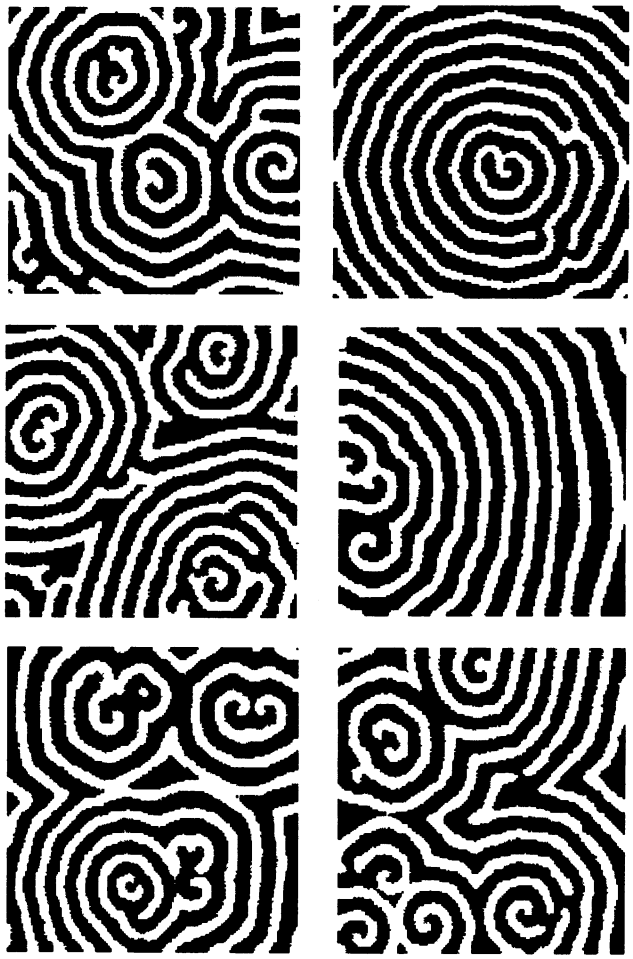

FIG. 3. A set of fully evolved spiral fields (time 20000) starting from different seeds of the random number generator controlling the random firing.

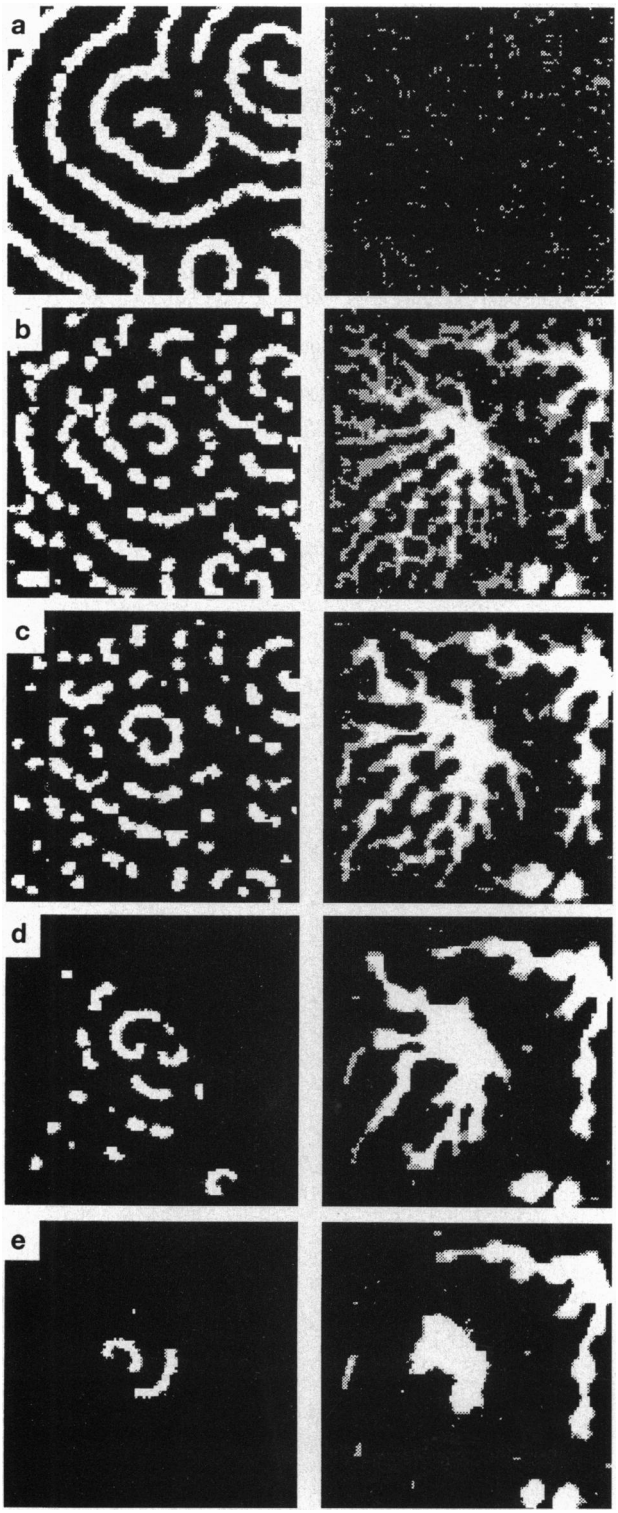

FIG. 4. A sequence of snapshots of cAMP concentration (*Left*) and cell density (*Right*) obtained by turning on chemotaxis in the model once the spiral wave field is established. The parameters for this simulation are the same as for Fig. 2 with the exception of density = 0.85, $\alpha = 0.009$, $\beta = 0.64$, $E_{max} = 0.87$, snapshots *a–e* were taken at $T = 2250, 3000, 5000, 15000$, respectively.

spiral cores and the excitability field E. We have checked that this spiral coarsening effect is a robust feature of the simulation, in the sense that its occurrence does not depend on any of the many specific assumptions and parameter values which characterize our model. The detailed final state of the process depends of course on the detailed initial firing pattern, leading to a variety of possible structures (Fig. 3); however, all of these have the same general structure and agree with the general structure seen experimentally.

Thus, the simplest prediction that comes out of our work is that a coherent spiral pattern cannot be obtained without this type of positive feedback. As we have stressed, the best candidate for this feedback is the known genetic coupling. Hence, mutant strains that "break" this connection should show either concentric cAMP waves (if the excitability is always high, such as by constitutive expression of the cAMP signaling system) or small scale spiral turbulence (if excitability increases in a spatially uniform manner). It might also be possible to test this idea without generating new mutant strains. Remixing of chemotactically deficient cells after development of full excitability should also suffice, although one would need to check that the pattern again starts through random firing. We note that for simplicity our computational model of increased excitability has kept fixed the amount of cAMP released per cell and lowered the signal threshold. Biologically, this occurs through an increase in the number of CAR1 receptors, but the positive feedback loop also affects adenyl cyclase expression and hence the emission increases as well. Within our simulation, these effects are functionally interchangeable and hence we predict that the wave patterns should be unable to distinguish between different molecular contributions to changes of excitability.

As already mentioned, at some point in the signaling process, cells began to move chemotactically (22) towards wave sources. The large coherent spirals delimited the territory that will eventually be incorporated into one mound. If we include chemotactic motion within our model, this phenomenon can be directly visualized by monitoring the cell density field (Fig. 4). Each large spiraling region gives rise to one aggregate, with the cells approaching the center along high density streams. As the uniform density state broke up, the cAMP waves became focused along the streams and the spatial coherence of the waves diminished. Note that the spirals often persist in the nascent mounds; these rotate and send waves down the incoming streams. These simulations agree quite well with the expected cAMP wave structure inferred via darkfield microscopy (23). Given our results, this implies that the genetic feedback might be an evolutionary adaptive feature which enables the colony to increase the typical number of cells per aggregate so as to be able to more effectively complete the developmental program.

To summarize, we have shown how one can simulate the emergence of large spiral wave domains of cAMP signaling in *Dictyostelium* by incorporating the developmental kinetics of the cell excitability. Of particular interest is the fact that positive feedback from cAMP signal reception to gene expression is of critical importance for organizing the aggregation pattern. This direct coupling of genetic expression to spatial pattern formation so as to cause an instability (spiral coarsening) in the latter has not been previously proposed as an important developmental mechanism; nonetheless, such an interaction might be a common strategy in developmental biology.

We would like to acknowledge useful conversations with R. Goldstein, D. Kessler, W. Loomis, G. Shaulsky, and E. Cox. This work was supported in part by National Science Foundation Grant DMR94-15460 (H.L.) and Department of Energy Grants DE-FG03-95ER14516 and DE-FG03-96ER14592 (L.T.). The work of I.A. was partially supported by the Raschi Foundation. I.A. acknowledges the hospitality of the Institute for Nonlinear Science, UCSD. T.V.T. acknowledges the support of the National Science Foundation through its Research Experience for Undergraduates program for undergraduate research.

1. Loomis, W. F., ed. (1992) *The Development of Dictyostelium discoideum* (Academic, San Diego).

2. Newell, P. C. (1981) in *Biology of the Chemotactic Response*, ed. Lackie, J. M. (Cambridge Univ. Press, Cambridge, U.K.).
3. Skinner, G. S. & Swinney, H. L. (1991) *Physics D* **48,** 1–16.
4. Jakubith, S., Rotermond, H. H., Engel, W., Von Oertzen, A. & Ertl, G. (1990) *Physics Rev. Lett.* **65,** 3013–3016.
5. Tomchik, K. & Devreotes, P. (1981) *Science* **212,** 443–446.
6. Alacantra, F. & Monk, M. (1974) *J. Gen Microbiol.* **85,** 321–334.
7. Devreotes, P. N. (1994) *Neuron* **12,** 235–241.
8. Vaughan, R. A. & Devreotes, P. N. (1988) *J. Biol. Chem.* **263,** 14538–14543.
9. Franke, J. M., Faure, M., Wu, L. L., Hall, A. L., Podgorski, G. J. & Kessin, R. H. (1991) *Dev. Genet.* **12,** 104–112.
10. Kimmel, A. R. & Firtel, R. A. (1991) *Curr. Opin. Genet. Dev.* **1,** 383–386.
11. Kessler, D. A. & Levine, H. (1993) *Phys. Rev. E* **48,** 4801–4804.
12. Levine, H. (1994) *Chaos* **4,** 563–568.
13. Martiel, J.-L. & Goldbeter, A. (1983) *Biophys. J.* **52,** 807–828.
14. Tang, Y. & Othmer, H. B. (1994) *Math. Biosci.* **120,** 25–76.
15. Weimar, J. R., Tyson, J. J. & Watson, L. T. (1992) *Physica D* **55,** 309–327.
16. Tyson, J. J., Alexander, K. A., Manoranjan, V. S. & Murray, J. D. (1989) *Physics D* **34,** 193–207.
17. Vasiev, B. N., Hogeweg, P. & Panfilov, A. V. (1994) *Phys. Rev. Lett.* **73,** 3173–3176.
18. Hofer, T., Sherratt, J. A. & Maini, P. K. (1995) *Proc. R. Soc. London B* **259,** 249–257.
19. Rathi, A., Kayman, S. C. & Clarke, M. (1991) *Dev. Genet.* **12,** 82–87.
20. Maselko, J. & Showalter, K. (1991) *Physica D* **49,** 21–32.
21. Aranson, I., Levine, H. & Tsimring, L. (1996) *Phys. Rev. Lett.*, **76,** 1170–1173.
22. Wessels, D., Murray, J. & Soll, D. R. (1992) *Cell Motil. Cytoskel.* **23,** 145–156.
23. Siegert, F. & Weijer, C. (1995) *Curr. Biol.* **5,** 937–943.